COBEM 99
XV Congresso Brasileiro de Engenharia Mecânica
15th Brazilian Congress of Mechanical Engineering
22 - 26 de Novembro de 1999 / November 22 - 26, 1999 Águas de Lindóia, São Paulo,

STUDY OF THE ASPECT RATIO EFFECT IN A THERMALLY-DRIVEN OPEN CAVITY

Admilson Teixeira Franco
Federal Center for Education in Technology - CEFET - PR
Department of Mechanical Engineering - DAMEC
Concurrent Engineering R & D Laboratory - NuPES
Av. Sete de Setembro, 3165
80230-901 - Curitiba - PR - Brazil

Marcelo Moreira Ganzarolli
State University of Campinas - UNICAMP
Mechanical Engineering Faculty - FEM, Energy Department - DE
Cidade Universitária Zeferino Vaz
13081-970 - Campinas - SP - Brazil

Summary. *Natural convection in a thermally-driven open cavity is analysed numerically. The vertical wall is heated and the horizontal walls are adiabatic. The other vertical wall is open to a fluid reservoir. Laminar and two-dimensional flow is assumed for Rayleigh number ranging from* 10^3 *to* 10^7*. The fluid is aproximately air with Prandtl number fixed at 1.0. The problem is solved numerically by using the Finite Volume-SOLA method. The average Nusselt number is reported for different values of the Rayleigh number. The aspect ratio of the open cavity is done as* $L/H = 0.5$*, 1.0, 3.0 and 6.0, where* L *is the cavity width and* H *is the cavity height. The main characteristics of the flow and the heat transfer process is discussed.*

Key-words: *Natural convection, Aspect ratio effect, Open cavity*

1. INTRODUCTION

Natural convection phenomenon in closed cavities has been intensively studied in the last years. We can report the works Hortmann *et al.* (1990) e Lé Quére (1991). However, natural convection in open cavities which has many practical applications, namely, building insulation, solar cavity receivers and cooling of electronic components has received less attention. In the numerical papers related to this subject, Chan e Tien (1985a), Chan e Tien (1985b), Angirasa *et al.* (1992) and Mohamad (1995) limited their computational domain to within the cavity without considers the region around of the opening, where is difficult to impose the boundary conditions. For low Rayleigh numbers, it is necessary to extend the computational domain beyond the opening. Thus, the Nusselt number will

not be affected.

As showed in Fig. 1, the cavity has both horizontal walls adiabatic and the vertical one is maintained heated. The flow is generated by the variations in the density around the heated wall.

The proposed geometry was solved by Chan e Tien (1985a) for Rayleigh number ranging from $10^3 - 10^9$ using a unity Prandtl number. They found that for high Rayleigh numbers, $Ra > 10^6$, it seems a recirculation zone on the bottom wall, due the incoming flow turning around the corner. The external region near the opening need to be considerated in order to model the problem properly. The aspect ratio of the open cavity was $B = 1.0$. An aspect ratio $B = 7.0$ was studied by Chan e Tien (1985b). In that work they examine the effect of the imposition of the boundary conditions in the opening of the cavity versus an extended domain. They concluded that it is reasonable to use the first condition for the shallow cavity, and that it is possible to foresee the main heat transfer characteristic parameters.

Angirasa *et al.* (1992) studied the problem using the Vorticity-Stream Function method and the computational domain confined to within the open cavity. They include a discussion about the boundary condition specification for the vorticity and the stream function in the opening.

A laminar solution for Rayleigh number in the range $10^3 - 10^7$ was done by Mohamad (1995). He reports results for the cavity inclination and the aspect ratio $B = 0.5$, 1.0 e 2.0. He found that the local Nusselt numbers is very sensible to the cavity inclinations and it promoves little variations on the average Nusselt number. The flow is instable for high Rayleigh numbers and for little cavity inclinations. All the results are obtained with the computational domain confined to the cavity. The region outside of the cavity is not considered in the solution.

The purpose of this work is to discuss the aspect ratio effect $B = 0.5$, 1.0 e 3.0 and 6.0 in the heat transfer process from the heated vertical wall inside the cavity. The computational domain was extended so it was not necessary to specify the boundary conditions in the opening.

2. PROBLEM FORMULATION

The cavity geometry and the boundary conditions are showed in Fig. 1. The open cavity is the $L \times H$ domain. The extended domain is the region $b \times Z$, where $Z = 5H$. The vertical wall inside the cavity is mantained at constant temperature T_h and the fluid reservoir (or ambient) at T_o. Laminar flow is assumed and the Boussinesq approximation is considerated valid. The dimensionless variable are defined below.

$$(X, Y) = \frac{(x, y)}{H} \tag{1}$$

$$(U, V) = \frac{(u, v)H}{\alpha} \tag{2}$$

$$\tau = \frac{\alpha t}{H^2} \tag{3}$$

$$T = \frac{T^\circ - T^\circ_\infty}{(T^\circ_h - T^\circ_\infty)} \tag{4}$$

$$P = \frac{(p - p_\infty)H^2}{\rho\alpha^2} \tag{5}$$

where T° indicates the dimensional temperature value.

Using the variables above, one can write the dimensionless conservation equation for mass, momentum and energy in transient form as

$$\frac{\partial U}{\partial X} + \frac{\partial V}{\partial Y} = 0 \tag{6}$$

$$\frac{\partial U}{\partial \tau} + \frac{\partial (U^2)}{\partial X} + \frac{\partial (VU)}{\partial Y} = -\frac{\partial P}{\partial X} + Pr\left(\frac{\partial^2 U}{\partial X^2} + \frac{\partial^2 U}{\partial Y^2}\right) \tag{7}$$

$$\frac{\partial V}{\partial \tau} + \frac{\partial (UV)}{\partial X} + \frac{\partial (V^2)}{\partial Y} = -\frac{\partial P}{\partial Y} + Pr\left(\frac{\partial^2 V}{\partial X^2} + \frac{\partial^2 V}{\partial Y^2}\right) + Ra.Pr.T \tag{8}$$

$$\frac{\partial T}{\partial \tau} + \frac{\partial (UT)}{\partial X} + \frac{\partial (VT)}{\partial Y} = \left(\frac{\partial^2 T}{\partial X^2} + \frac{\partial^2 T}{\partial Y^2}\right) \tag{9}$$

where the quantities $Pr = \nu/\alpha$ and $Ra = g\beta H^3(T_h^\circ - T_\infty^\circ)/\alpha\nu$ are the Prandtl and the Rayleigh numbers, respectively.

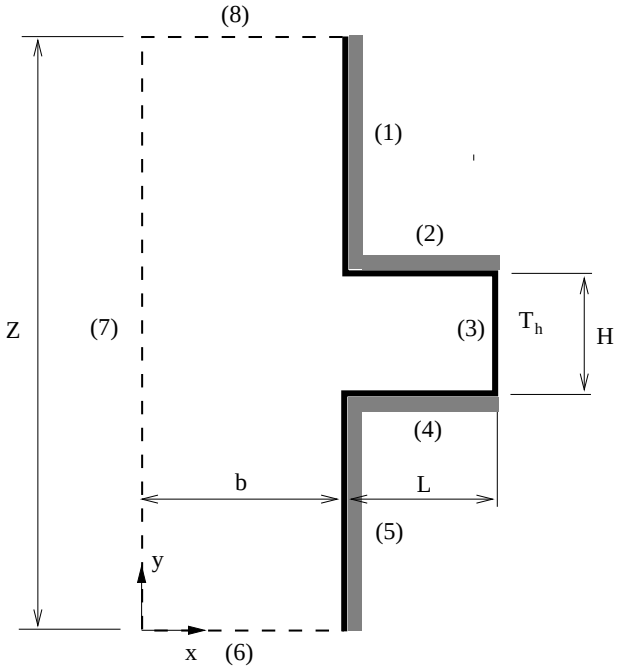

Figure 1: Geometry and the coordinate system

The boundary conditions at the borders showed in Fig. 1 are

- (1) $U = V = \partial T/\partial X = 0$
- (2) $U = V = \partial T/\partial Y = 0$
- (3) $U = V = 0$ e $T = 1$

- (4) $U = V = \partial T/\partial Y = 0$
- (5) $U = V = \partial T/\partial X = 0$
- (6) $(\partial U/\partial Y) = V = T_{in} = 0$
- (7) $U = V = (\partial T/\partial X = 0)_{out}$ ou $T_{in} = 0$
- (8) $(\partial U/\partial Y) = (\partial V/\partial Y) = (\partial T/\partial Y)_{out} = 0$

The average Nusselt number on the hotted wall, $\overline{Nu}$, is defined as

$$\overline{Nu} = \int_0^1 \left(\frac{\partial T}{\partial X}\right)_{X=0} dY = \overline{Nu}(Ra, Pr, B) \tag{10}$$

The dimensionless stream function is

$$\Psi(X,Y) = -\int_{X_o}^{X} V(X,Y)dX + \Psi(X_o, Y_o) \tag{11}$$

where the value $\Psi(X_o, Y_o)$ is zero in the solid walls.

The volumetric mass rate is defined as

$$\dot{m} = \int_{Opening} U_{in} dY \tag{12}$$

$$\begin{aligned} U_{in} &= U_{X=b/H} \quad \text{if} \quad U_{X=b/H} > 0 \\ U_{in} &= 0 \qquad\quad \text{if} \quad U_{X=b/H} \leq 0 \end{aligned}$$

3. NUMERICAL PROCEDURE

The equations above are discretized using the Finite Volume Method (Patankar, 1980) for the spatial discretization and the SOLA method for the time discretization (Hirt *et al.* (1975)). The SOLA method consists of advancing in the time the velocity and the pressure fields from a previous values of velocities, stopping the procedure when convergence criteria is reached

$$\max \left| \frac{\phi^{n+1} - \phi^n}{\phi^{n+1}} \right| < 10^{-5} \tag{13}$$

onde $\phi = U, V, T$ e Nu.

The numerical code was validated by checking this with the Chan e Tien (1985b) results. For example, at $Ra = 10^6$ and using 21×21 points inside the cavity, the values obtained for $\overline{Nu}$ and $\dot{m}$ are 15.0 and 47.3 against 15.0 and 47.6 obtained by Chan e Tien (1985b).

For an aspect ratio like as B =1.0 and $Ra = 10^5$, when the points inside the cavity is increased from 21×21 to 31×31, the Nusselt number variation is less than 0.2%.

4. RESULTS AND DISCUSSION

In this section is showed the effects of the aspect ratio B = 0.5, 1.0, 3.0 and 6.0 and the Rayleigh number ranging from $10^3 - 10^7$, in the heat transfer process from the

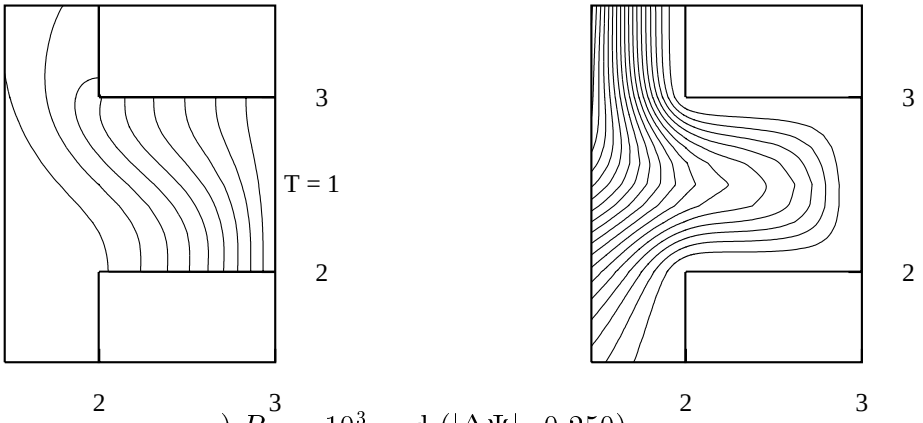

a-) $Ra = 10^3$ and ($|\Delta\Psi|$=0.250)

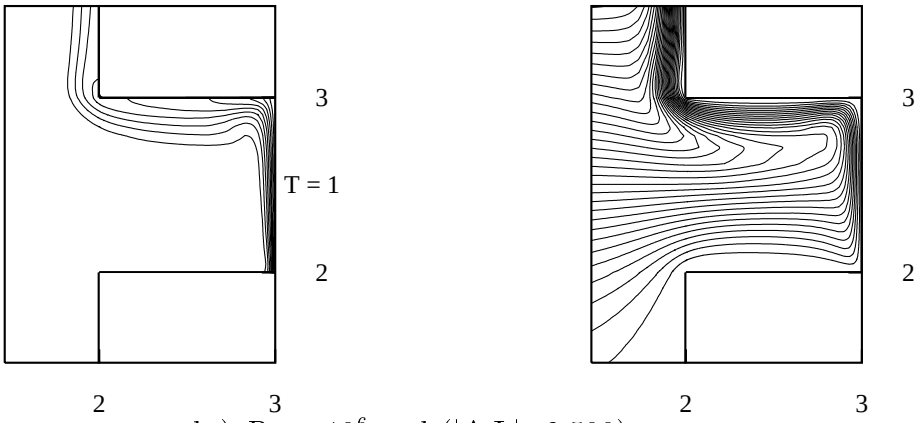

b-) $Ra = 10^6$ and ($|\Delta\Psi|$=2.500)

Figure 2: Isothermals and streamlines for $B = 1.0$

heated vertical wall of the open cavity. An unit Prandtl number is considered, which is aproximately air.

In the following figures, the contour maps showing the isotherms and the streamlines were plotted. The intervals between the isotherms are always $\Delta T = 0.1$ and for the streamlines it is showed together with the figure. Only the region near of the open cavity is showed.

Figures 2, 3 and 4 show the isotherms and streamlines for $B = 1.0$, 3.0 and 6.0. In each figure, we show in letter a-) the results for $Ra = 10^3$ and in letter b-) the results for $Ra = 10^6$, characterizing the conduction limit and the boundary layer regime, respectively. The results for $B = 0.5$ are not plotted because they seem like the one for $B = 1.0$. The differences are that for $B = 0.5$, the hotted wall affect a larger region near the opening.

Figures 2a, 3a and 4a show the isotherms and streamlines for $Ra = 10^3$. We can see that the conduction is the dominant heat transfer mechanism. When the cavity becomes deeper, the isotherms are distribuited along the cavity and the streamlines pattern are symmetric and similar.

Figures 2b, 3b and 4b show the isotherms and streamlines for $Ra = 10^6$. As we can see, in this case appears near of the hotted wall the boundary layer strucuture. The fluid penetrates into the cavity and is acelerated by the hotted vertical wall, leaving the cavity

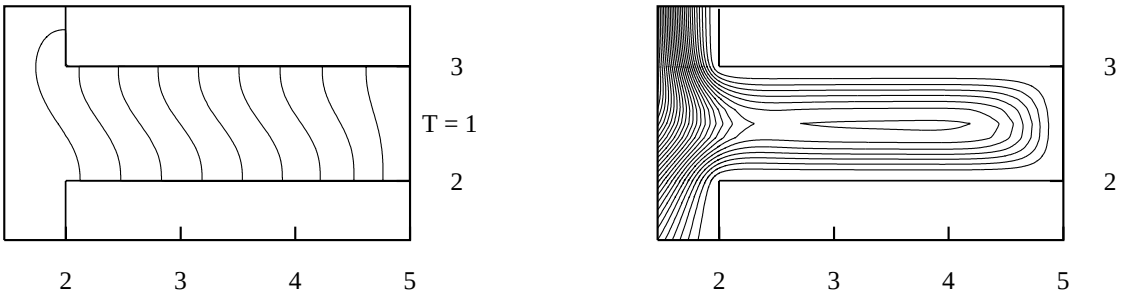

a-) $Ra = 10^3$ and $|\Delta\Psi|$=0.100

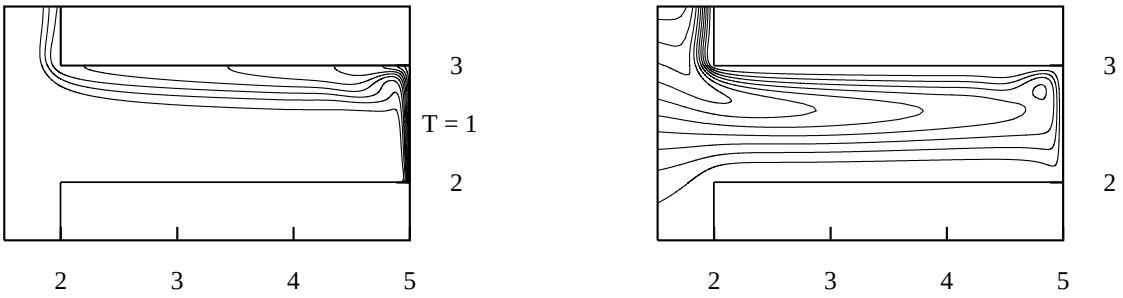

b-) $Ra = 10^6$ and $|\Delta\Psi|$=7.500

Figure 3: Isothermals and streamlines for $B = 3.0$

adjacent to the upper horizontal adiabatic wall.

From a thermal engineering standpoint, two other characteristics are very important, namely, the average Nusselt number of the hotted vertical wall, $\overline{Nu}$, and the volumetric flow rate, $\dot{m}$, entering into the cavity. Fig. 5 shows the Rayleigh number effect on the average Nusselt number as function of the aspect ratio B. We can see that the behaviour of $B = 0.5$ and $B = 1.0$, have the same aspect. For Ra higher than 10^5, every cases are analogous to the vertical flat plate behaviour, as is showed by the $Ra^{1/4}$ scale. For the conduction limit, $Ra = 10^3$, the Nusselt number can be write just a function of the aspect ratio

$$\overline{Nu} \cong \frac{H}{L} = (B)^{-1} \tag{14}$$

When $Ra \geq 10^6$, the $\overline{Nu}$ is independent of the aspect ratio, because the convective effects generated by the boundary layer is the dominant heat transfer mechanism.

Figure 6 represents the volumetric flow rate entering into the open cavity, $\dot{m}$. While the convection is not dominant, $Ra < 10^5$ and the cavity becomes deeper, less flow is entering by the opening. Otherwise, when $Ra > 10^5$, the depth cavity induces more mass into the cavity. When B increases, the flow enteres horinzontally into the cavity and as result, the $\dot{m}$ is bigger.

Figure 7 shows the U velocity component profile and the temperature profile in the exit of the cavity, for Rayleigh number 10^3, 10^5 and 10^7, respectively. When the Rayleigh number is low, $Ra = 10^3$, Figure 7a, the velocity profile is practicely symmetric. Because the hotted wall has a longer distance from the opening, when B increases, the fluid

temperature is close to the fluid reservoir temperature.

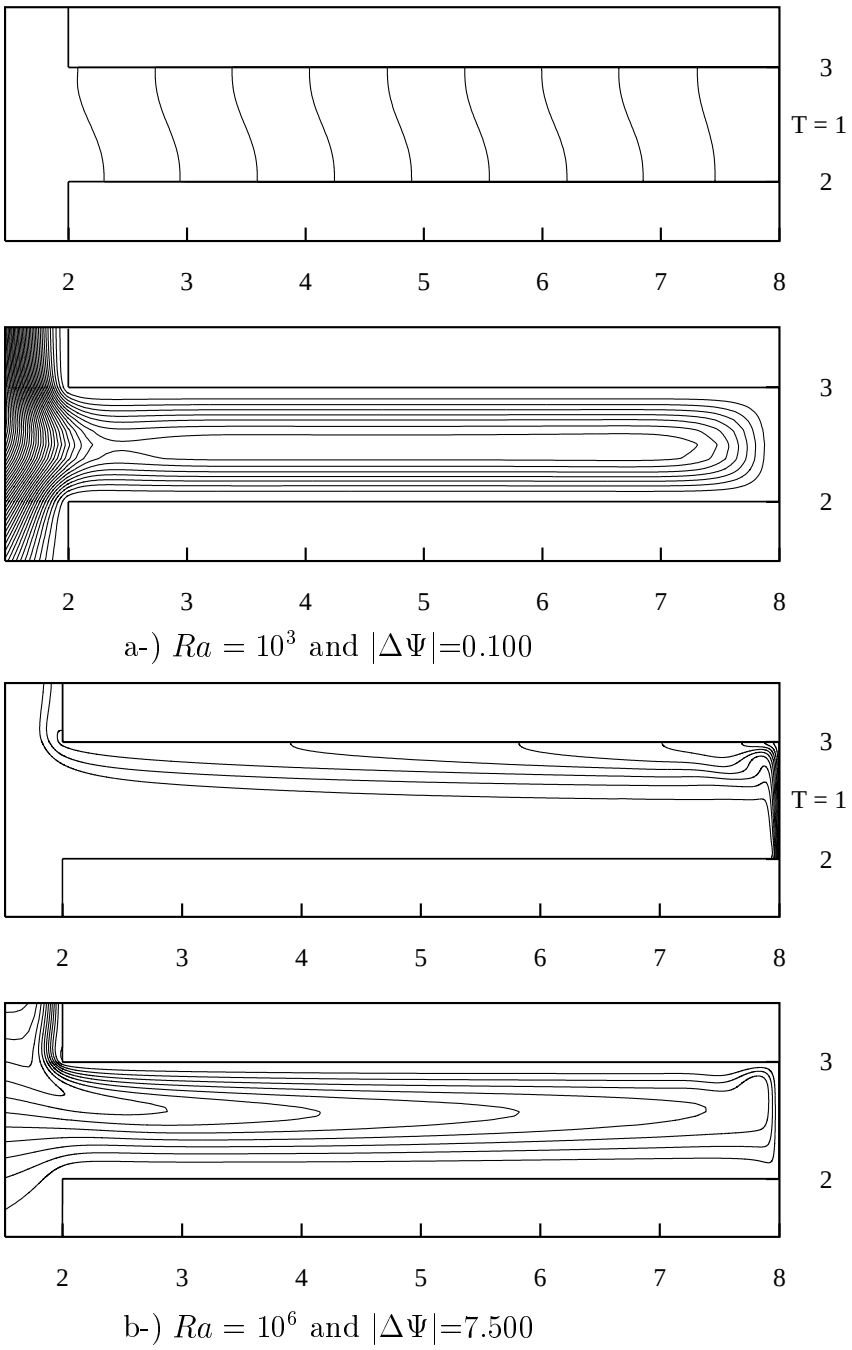

Figure 4: Isothermals and streamlines for $B = 6.0$

Figure 7a, 7b and 7c show the effect of the increase of the Rayleigh number. The fluid entering into the cavity occupies practicely 2/3 of the opening at $Ra = 10^5$ and 4/5 at $Ra = 10^7$. This situation occurs for all aspect ratios B. The fluid lying the upper horizontal wall lets the cavity forming a jet. Such jet turns right the upper corner and ascends near the vertical wall.

For $Ra = 10^5$ and $Ra = 10^7$, the temperature profile shows that in the openingt, the fluid temperature of the flow entering into the cavity has nearly the fluid temperature of the reservoir, $T_o = 0$. On the upper horizontal adiabatic wall appears a high temperature gradient, Fig. 7c.

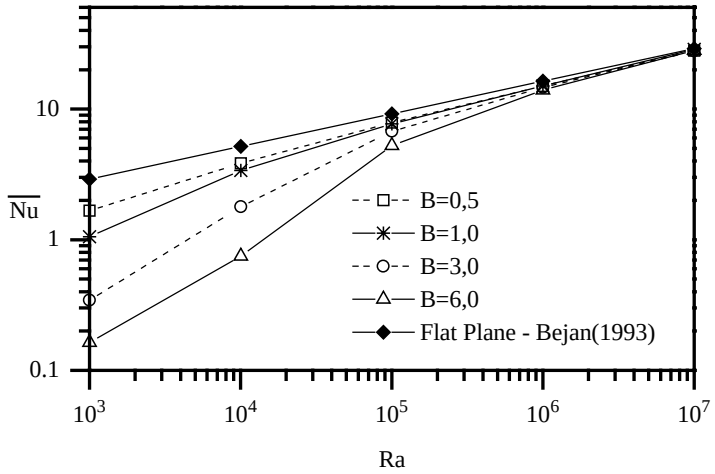

Figure 5: Rayleigh number effect on the average Nusselt number

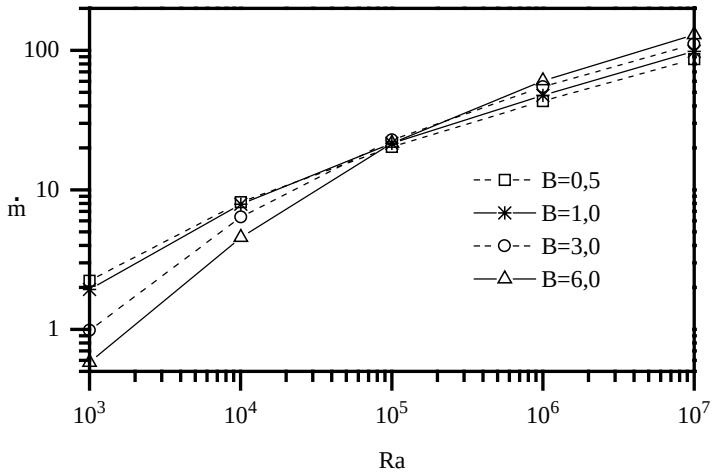

Figure 6: Rayleigh number effect on the volumetric flow rate

5. CONCLUDING REMARKS

In this work we studied natural convection in a thermally-driven open cavity. We studied the aspect ratio $B = L/H = 0.5$, 1.0, 3.0 and 6.0 and the Rayleigh number effects ranging from $10^3 - 10^7$.

When $Ra \geq 10^5$, the boundary layer appears on the vertical heated wall and the average Nusselt number follows the power-law $Ra^{1/4}$, which is validated for boundary layer on a vertical flat plate. For the conduction limit, when $Ra \leq 10^3$, the average Nusselt number is expressed by the Eq. (14), $\overline{Nu} \cong H/L = (B)^{-1}$.

The domain $Ra \times \dot{m}$ has the value $Ra = 10^5$ as a point where the curves for the aspect ratios change the slop.

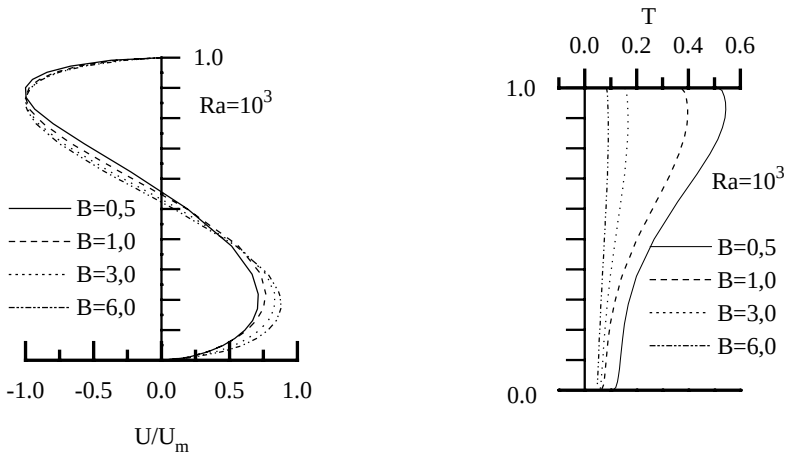

a-)

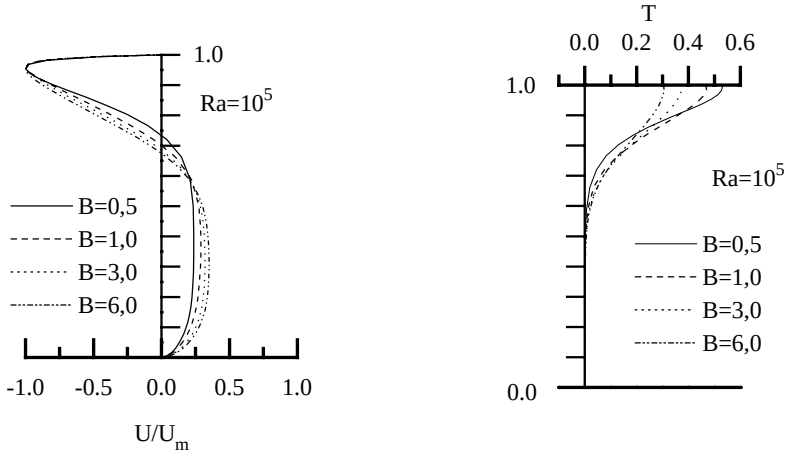

b-)

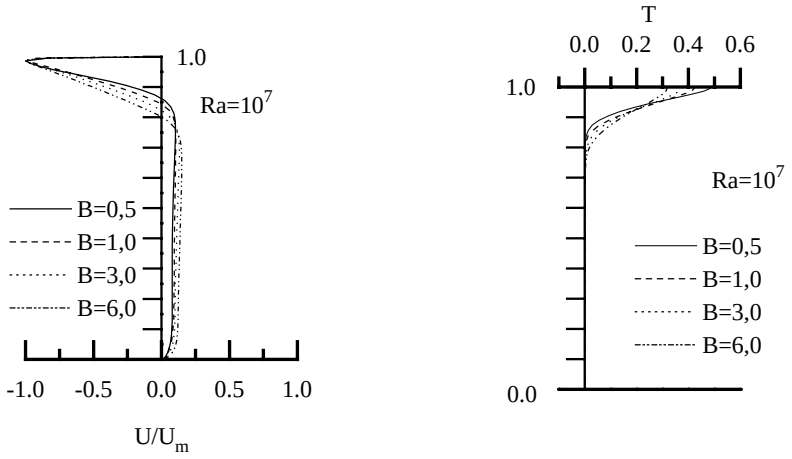

c-)

Figure 7: U velocity component and temperature profile in the opening

6. REFERENCES

Angirasa, D., Eggels, J. E. M. e Niewstadt, F. T. M., 1995, Numerical Simulation of Transient Natural Convection from a Isothermal Cavity Open on a Side, *Numerical Heat Transfer*, Vol. 28, Parte A, p. 755-768.

Angirasa, D., Pourquié, M. J. B. M. e Niewstadt, F. T. M., 1992, Numerical Study of Transient and Steady Laminar Buoyancy-Driven Flows and Heat Transfer in a Square Open Cavity, *Numerical Heat Transfer*, Vol. 22, Parte A, p. 223-239.

Bejan, A., 1993, *Heat Transfer*, John Wiley & Sons, USA.

Bejan, A., 1994, *Convection Heat Transfer*, John Wiley & Sons, 2ª edição , USA.

Chan, Y. L. e Tien, C. L., 1983, Laminar Natural Convectiopn in a Shallow Open Cavities, *21st ASME-AIChe National Heat Transfer Conference - Natural Convection in Enclosures*, HTD, Vol. 26, p. 77-82.

Chan, Y. L. e Tien, C. L., 1985a, A Numerical Study of Two-Dimensional Natural Convection in a Square Open Cavities, *Numerical Heat Transfer*, Vol. 8, p. 65-80.

Chan, Y. L. e Tien, C. L., 1985b, A Numerical Study of Two-Dimensional Laminar Natural Convection in a Shallow Open Cavities, *International Journal Heat Mass Transfer*, Vol. 28, nº 3, p. 603-612.

Chan, Y. L. e Tien, C. L., 1986, Laminar Natural Convection in a Shallow Open Cavities, *Journal of Heat Transfer*, Vol. 108, p. 305-309.

Harlow, F. H. e Welch, J. E., 1965, Numerical Calculation of Time-Dependent Viscous Incompressible Flow of Fluid with Free Surface, *Physics of Fluids*, Vol. 8, p. 2182-2189.

Hirt, C. W., Nichols, B.D. and Romero, N.C., 1975, SOLA- Numerical Solution Algorithm for Transient Fluid Flow, *Los Alamos Laboratory*, Report LA-5852.

Hortmann, M., Peric, M. e Scheuerer, G., 1990, Finite Volume Multigrid Prediction of Laminar Natural Convection: Bench Mark Solution, *International Journal for Numerical Methods in Fluids*, Vol. 11, p. 189-207.

Lé Quére, P., 1991, Accurate Solutions to the Square Thermally Driven Cavity at High Rayleigh Number, *Computer Fluids*, Vol. 20, nº 1, p. 29-41.

Mohamad, A. A., 1989, Natural Convection in Open Cavities and Slots, *Numerical Heat Transfer*, Vol. 27, Parte A, p. 705-716.

Patankar, S. V., 1980, *Numerical Heat Transfer and Fluid Flow*, Hemisphere Publishing Corporation, USA.